Applied Catalysis A: General 390 (2010) 264–270

Contents lists available at ScienceDirect

Applied Catalysis A: General

journal homepage: www.elsevier.com/locate/apcata

Dehydrogenation of propane over Pt/KL catalyst: Investigating the role of L-zeolite structure on catalyst performance using isotope labeling

Khalid G. Azzam, Gary Jacobs, Wilson D. Shafer, Burtron H. Davis*

Center for Applied Energy Research, University of Kentucky, 2540 Research Park Drive, Lexington, KY 40511, USA

ARTICLE INFO

Article history:
Received 11 June 2010
Received in revised form 13 October 2010
Accepted 20 October 2010
Available online 27 October 2010

Keywords:
Dehydrogenation
Propane
C_3H_8
C_3D_8
Pt/KL
L-zeolite
Isotope effect
Diffusion
H–D exchange

ABSTRACT

Dehydrogenation of propane using an equimolar mixture of propane-d_0 and propane-d_8 was investigated over 1%Pt/KL and 1%Pt/SiO_2 at atmospheric pressure and different reaction temperatures. A normal kinetic isotope effect exists ($k_H/k_D = 1.4–1.5$) when the reaction is conducted on Pt/KL at different temperatures (400, 500, and 600 °C), suggesting that C–H bond activation is involved in the kinetically relevant steps. Furtheremore, there is hardly any H–D exchange in the recovered propane during dehydrogenation at temperatures above 400 °C, suggesting that adsorption and subsequent dehydrogenation of propane are essentially irreversible and that C–H bond activation is the rate determining step. Unlike the case of hexane aromatization, the unique structure of L-zeolite does not help in controlling the entry of propane molecules into the lobes of the L-zeolite containing the active sites; hence, bimolecular reactions do occur, leading to coke formation and catalyst deactivation.

1. Introduction

Dehydrogenation of propane to propylene is an important reaction, since propylene is a vital feedstock in the petrochemical industry. The majority of propylene is produced as a by-product from processes such as steam cracking of naphtha and fluid catalytic cracking (FCC) [1]. However, due to increased global demand, several new plants for the dehydrogenation of propane to propylene have been built worldwide [1]. Dehydrogenation of propane is a highly endothermic reaction favored by high temperatures and low hydrogen partial pressures. Typically, Pt–Sn supported on alumina or Cr_2O_3 supported on alumina or zirconia are the commercial catalysts for this reaction [1,2]. A variety of Pt catalysts, often promoted with other electropositive metals and supported on various carriers (e.g., SiO_2 [3], ZSM5 [4,5], L-zeolite [6], SBA-15 [2,5,7], Y-zeolite [6], MOR [6], Beta [6,8], and Mg(Al)O [9]), were investigated for the dehydrogenation of propane to propylene reaction in an effort to find an optimum catalyst.

Over Pt, alkane dehydrogenation requires elementary steps including activation of the C–H bond and elimination of the hydrogen formed. Due to the lower reactivity of the C–D bond relative to C–H in alkanes, isotopic switching can be used to determine if a normal kinetic isotope effect (NKIE) exists which would suggest C–H bond breaking as the rate limiting step among the elementary steps. Furthermore, the degree of H–D scrambling in the recovered-unreacted alkanes [10–13] provides important information regarding the extent of reaction of the alkane reactant with the surface hydrogen pool. Jackson et al. [14] studied the dehydrogenation of propane using a C_3H_8/C_3D_8 mixture on chromia and found an NKIE of 1.85; thus, C–H bond activation was identified to be the rate determining step. Biscardi and Iglesia [15] investigated the elementary reaction steps of propane dehydrogenation over H-ZSM5 and Ga/H-ZSM5 catalysts using an equimolar mixture of C_3H_8/C_3D_8. At a temperature of 500 °C, an NKIE of 1.03 and 1.2 for H-ZSM5 and Ga/H-ZSM5, respectively, were reported and significant H–D cross-exchange between C_3H_8 and C_3D_8 in the recovered propane was observed. Therefore, they [15] concluded that the C–H bond activation step does not limit the overall dehydrogenation rate and H–D exchange is strongly influenced by the Bronsted acid sites on those catalysts. Recently, we [16] have found using isotope labeling that the unique structure of L-zeolite plays a significant role in controlling the entry of hexane molecules into the wider lobes of L-zeolite containing the Pt active sites during the dehydrocyclization reaction; in that case, the catalyst was prepared by chemical vapor deposition (CVD) of $Pt(AcAc)_2$ to ensure that ultra-small Pt clusters were formed, situated inside the uni-

---

* Corresponding author. Tel.: +1 859 257 0253; fax: +1 859 257 0302.
E-mail address: davis@caer.uky.edu (B.H. Davis).

0926-860X/$ – see front matter © 2010 Elsevier B.V. All rights reserved.
doi:10.1016/j.apcata.2010.10.022

axial channels and with a majority nestled within the wider lobes. Because of this unique property, the catalyst exhibited unparalleled stability for hexane aromatization, as bimolecular reactions leading to coking were avoided [15,16]. Since Pt supported on L-zeolite is reported to be a promising catalyst for the dehydrogenation of alkanes to alkenes [6,17,18], it is important to investigate if the unique structure of L-zeolite can play a role in those Pt-catalyzed reactions as well. Using propane as the reactant, the aim of this study is to determine if an NKIE exists and to investigate the extent to which intracrystalline diffusion plays a role in the dehydrogenation of lighter alkanes; this is accomplished by carrying out experiments using an equimolar ratio of C_3H_8 and C_3D_8 in the feed.

2. Experimental

2.1. Catalyst preparation

A sample of potassium exchanged zeolite LTL (Süd-Chemie) was calcined in flowing air (100 cm^3/min) at 400 °C for 4 h. After cooling to ambient temperature, the calcined zeolite LTL powder was transferred to a glove bag filled with inert gas and carefully mixed with platinum acetylacetonate (Alfa Aesar); the material was then loaded into a sublimation tube, which was sealed at one end. The other end was attached to a high vacuum system, equipped with an oil diffusion pump and capable of achieving a vacuum of $<10^{-6}$ Torr. The sublimation tube was held at room temperature for 4 h, and then the temperature was slowly ramped (1 °C/min) to 70, 80, 90, and then 100 °C, holding at each temperature for 1 h. Finally, the temperature was ramped to 130 °C, held for 15 min, and cooled to room temperature. Following the CVD procedure, the sample was light yellow in color. To decompose the $Pt(AcAc)_2$ compound, the catalyst was calcined at 350 °C in flowing air for 4 h. The final catalyst was light gray in color. The loading was 1%Pt by weight. Various sublimation methods for obtaining highly dispersed Pt/KL catalysts can be found in the literature [16–22].

The Pt/SiO_2 catalyst was prepared using the incipient wetness impregnation (IWI) method. Silica (The PQ Corporation, CS-2133) was used as the catalyst support. In this method, IWI of the support was performed with the Pt salt, tetraamineplatinum (II) nitrate (Alfa, Stock #88960, Lot #A29T027). The loading solution volume was determined based on the average pore volume of silica used. After impregnation, the sample was dried for 6 h at 110 °C and subsequently calcined in stagnant air at 350 °C (ramp of 3 °C/min) for 4 h.

2.2. Catalyst characterization

Hydrogen chemisorption by a temperature programmed desorption (TPD) method was carried out using a Zeton-Altamira AMI-200 unit. The catalyst was slowly heated (1 °C/min) to either 450, 500 or 600 °C in 30 cm^3/min of a 33%H_2/Ar mixture, and held at 450, 500 or 600 °C for 1 h. The catalyst was then cooled in flowing hydrogen to 80 °C, and purged with 25 cm^3/min of flowing argon to remove weakly bound hydrogen. The catalyst was then heated in 25 cm^3/min of flowing argon to 450, 500 or 600 °C to desorb the hydrogen, and the evolved hydrogen was monitored using a thermal conductivity detector (TCD). To calibrate the signal, 10 pulses of standard amounts of hydrogen were passed into a flowing argon stream.

Diffuse reflectance infrared Fourier transform spectroscopy (DRIFTS) spectra were recorded using a Nicolet Nexus 870 spectrometer equipped with a DTGS-TEC detector. A Thermo Spectra-Tech cell capable of high pressure/high temperature operation and fitted with ZnSe windows served as the reaction chamber for in situ CO adsorption measurements. Scans were taken at a resolution of 4 to give a data spacing of 1.928 cm^{-1}. The catalyst (~40 mg) was first activated at 450, 500 or 600 °C in 75 sccm 33%H_2/He for 1 h, purged with He for 15 min, and cooled to 40 °C in 50 sccm of He flow. To probe the Pt^0 clusters, the catalyst was subjected to 50 sccm of 2%CO/He at 40 °C for 30 min. The catalyst was then purged in 50 sccm He for 20 min. Scans were recorded during CO adsorption and following the He purge. A 1%Pt/SiO_2 catalyst, prepared by incipient wetness impregnation, served as the reference sample.

Temperature programmed oxidation (TPO) of the used catalysts was conducted using a stainless steel fixed-bed tubular reactor (0.38 in, i.d.) system in which the outlet stream was directed to a sampling valve on the gas chromatograph (SRI 8610C). The GC includes two columns (6′ silica gel packed and 3′ molecular sieve packed) and two detectors (FID and TCD). To boost the sensitivity of the CO and CO_2 signals, the GC incorporates a methanizer, such that these products can be analyzed by FID. The catalysts were heated in a 1% O_2/He stream from room temperature to 750 °C (heating rate 1 °C/min^{-1}). The reactor effluent was analyzed every 7 min.

2.3. Activity test

Catalytic tests for propane dehydrogenation were carried out using a stainless steel fixed-bed tubular reactor (0.38 in, i.d.) under steady state conditions. Typically, the catalysts were pressed into pellets, crushed, and sieved to yield grains 355–600 μm in diameter. A 400 mg catalyst sample was packed between two layers of quartz wool. The temperature of the catalyst bed was monitored using an internal thermocouple (Fe–Cr) and maintained by a temperature controller (Ω Omega CN 3251-R). Propane-d_0 (Scott Gross, 33%/He balance) and propane-d_8 (Cambridge Isotope Laboratories, 98% purity) were controlled by Brooks mass flow controllers to yield a mixture of 25% propane-d_0/25% propane-d_8/balance He. Prior to catalytic testing, the catalyst was reduced in H_2 at the reaction temperature (i.e., 500 or 600 °C for 15 min with a temperature ramp of 4 °C/min). For the experiments conducted at 300 and 400 °C, the catalyst was reduced in H_2 at 450 °C to ensure complete reduction of platinum to Pt^0. Reaction testing was conducted at a WHSV of 2.6 h^{-1} at atmospheric pressure and temperatures of 300, 400, 500, and 600 °C. A purge-valve was used to automatically direct samples to the GC for analysis. The feed and products were analyzed using an Agilent GC (7890A) which includes an HP-PLOT/Al_2O_3 'S' deactivated capillary column to achieve product separation. Products were detected using a flame ionization detector (FID). A linear 40 min temperature ramp from 35 to 180 °C provided the means for adequate peak separation in the GC column. Due to the good separation of propane-d_0 and propane-d_8 in the column (see Fig. 1), the conversions of both reactants were calculated using the FID data. The products were collected in sample bags and analyzed using an Agilent GC (6890)–MS (5973N) to investigate the extent of H-labeled hydrogen incorporation into the deuterated propane reactant, and likewise, the extent of D incorporation into the H-labeled propane reactant.

3. Results and discussion

The amounts of hydrogen evolved from the 1%Pt/KL CVD catalysts during sequential TPD were 51.5, 50.0, and 45.7 μmol/g, respectively, for the reduction temperatures of 450, 500, and 600 °C employed. These values correspond closely to a H/Pt ratio of ~2.0 (Table 1). Virtually identical results, obtained using the volumetric chemisorption approach, were reported previously [19,21], and indicate that the Pt clusters in the catalyst used in this work are extremely well-dispersed. Although H/Pt ratios above 1.0 are common in the literature [19,23,24] for Pt/KL catalysts, the CVD method

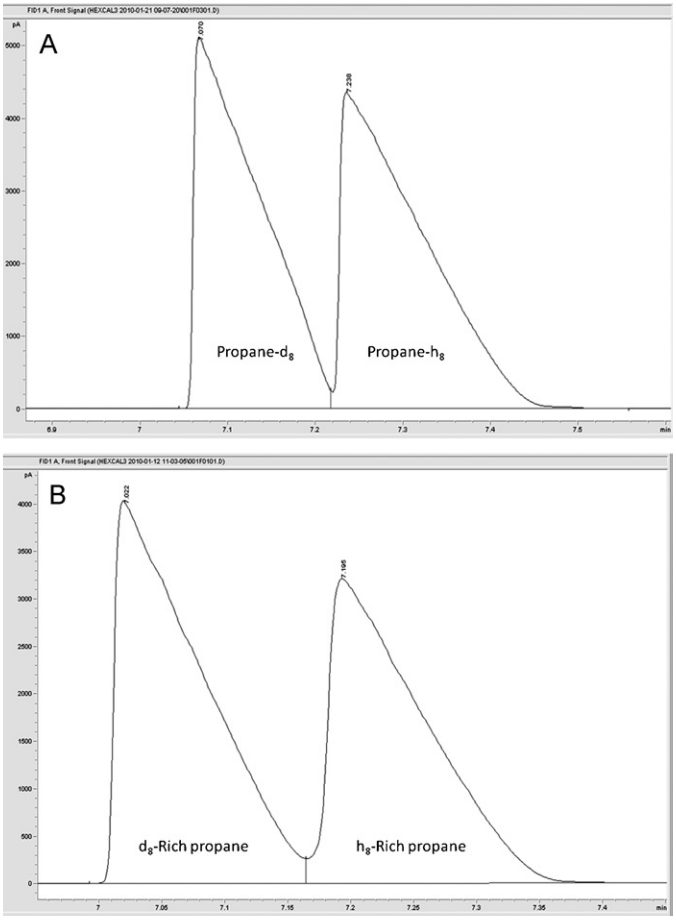

Fig. 1. FID gas chromatogram showing the efficiency of separating the propane-d_0 and propane-d_8 mixture using the HP-PLOT/Al_2O_3 'S' deactivated capillary column, (A) before reaction and (B) after reaction.

consistently yields among the highest dispersions. In the case of Pt/SiO_2, 27.1 μmol/g was evolved during the TPD measurments (see Table 1) corresponding to a H/Pt ratio of unity. The catalyst has high Pt dispersion with an average Pt particle size of about 1 nm. Despite the high dispersion of Pt particles in the case of Pt/SiO_2, they are still larger in size compared with those of the Pt/KL catalyst. Therefore, in the case of Pt/KL, not only are the particles considerably smaller than those reported for other methods (e.g., impregnation), but they generally exhibit greater spatial separations within the zeolite pores [19]. Indeed, conventional catalysts (e.g., prepared by incipient wetness impregnation or ion exchange, where particles are often clustered near the pore mouth [25]) typically exhibit an initial drop in conversion that is not observed with CVD catalysts. In a rigorous HR-TEM investigation, Treacy [26] found that after particle growth reaches a point where two or more channel blockages occur, a large fraction of Pt clusters become entrapped and the catalyst deactivates. However, the greater spatial separations of tiny Pt clusters within the pores of CVD catalysts prevent this from happening, and an initial drop is not observed [27]. Another testimony to this is that, even after high temperature treatment at 600 °C followed by H_2-TPD, though a slight decrease is observed compared to the TPD experiments carried out after 450 and 500 °C treatments, a very high dispersion is retained. Recall that the lobes are separated by narrow apertures such that if the Pt is well separated along the lengths of the channels (i.e., by employing the CVD method), then this geometry of the channel structure provides a physical activation energy barrier that inhibits particle migration and agglomeration.

Table 1
Physical and chemical characteristics of the catalysts.

Catalyst	S_{BET} (m^2/g)	Pore volume (m^3/g)	H/Pt[a]		
KL[b]	291	0.143	–	–	–
1 wt% Pt/KL[c]	190	0.100	2.01[d]	1.95[e]	1.78[f]
1 wt% Pt/SiO_2[c]	350	0.788	–	–	1.06[f]

[a] Measured by H_2 – TPD.
[b] Calcined at 400 °C.
[c] Calcined at 350 °C.
[d] Reduced in H_2 at 450 °C.
[e] Reduced in H_2 at 500 °C.
[f] Reduced in H_2 at 600 °C.

One method to verify the likelihood that the Pt^0 clusters are mainly within the zeolite channels is to use CO as a probe and follow the evolution of platinum carbonyl species by DRIFTS. These platinum carbonyl species are formed by the disruption of only highly dispersed Pt clusters by CO; they are stabilized by a ligand effect, proposed to be due to the interaction between electron-rich zeolite O atoms, located inside the zeolite channels, and the $Pt_x(CO)_y$ species [28,29]. Fig. 2A shows the Pt-carbonyl species evolved over the 1%Pt/KL CVD catalyst (solid line) and CO adsorption on a 1%Pt/SiO_2 reference catalyst (dashed line). Prior to recording the spectra, both catalysts were reduced in H_2 at 600 °C, in contact with CO for 30 min at 40 °C, and finally purged with He for 20 min. As can be seen, the majority of bands for 1%Pt/KL CVD are positioned at wave numbers much lower than the linear ν(CO) band observed for the typical 1%Pt/SiO_2 catalyst. The low wave number bands appear at discrete positions (bands at 2051, 2035, 2011, 1982, and 1962 cm^{-1}), suggesting that they likely correspond to $Pt_x(CO)_y$ species stabilized by the L-zeolite support. Although the DRIFTS results of adsorbed CO indicate that a high fraction of Pt resides inside the channels (Pt carbonyl bands ranging from 2051 cm^{-1} to 1962 cm^{-1}), there are also two shoulders present at 2084 and 2068 cm^{-1} for CO adsorbed on larger Pt metal crystallites. These particles are likely large enough to block the narrow window of the L-zeolite and therefore completely cut off reactant access to a fraction of the channels. The DRIFTS spectra for the catalysts reduced in H_2 at 600, 500, and 450 °C were fitted using a least squares fitting routine with Gaussian peaks (Fig. 2B–D, respectively). Two Gaussian peaks were used to define the ν(CO) of linearly bound CO on larger Pt crystallites (2068 cm^{-1} +) and five Gaussian peaks were used to define the ν(CO) bands of $Pt_x(CO)_y$ species stabilized by the KL zeolite (<2068 cm^{-1}), as depicted in Fig. 2B–D. For the cases of 450 and 500 °C reduction, approximately 20% of the linear stretching bands correspond to those assigned to CO adsorbed on larger Pt crystallites; the fraction is somewhat lower (~16%) for the case of 600 °C reduction due to the agglomeration of some of the larger particles—the bands at lower wave numbers being largely retained. This is consistent with a decrease in the BET surface area and pore volume by a fraction of ~1/3 (see Table 1) observed after Pt addition and calcination relative to KL zeolite alone. Nevertheless, DRIFTS results demonstrate that the majority of Pt is small enough, and in sufficent contact with the KL zeolite channels, to be converted to KL support-stabilized Pt carbonyl species upon CO adsorption (80–85% of the linear ν(CO) bands). Therefore, from the hydrogen chemisorption and DRIFTS results, one can conclude that the majority of Pt clusters are likely ultra-well-dispersed and located within the channels of the L-zeolite.

The relative conversions of propane-d_0 and propane-d_8 and the NKIE (k_H/k_D) versus time on-stream (TOS) during the dehydrogenation reaction of propane over the 1%Pt/KL at 600 °C, are shown in Table 2. It is obvious that the conversion of undeuterated propane is higher than that of deuterated propane over the testing interval. The NKIE (k_H/k_D) is greater than unity, with an average value of about 1.5 for all measured conversions over the testing interval. It is

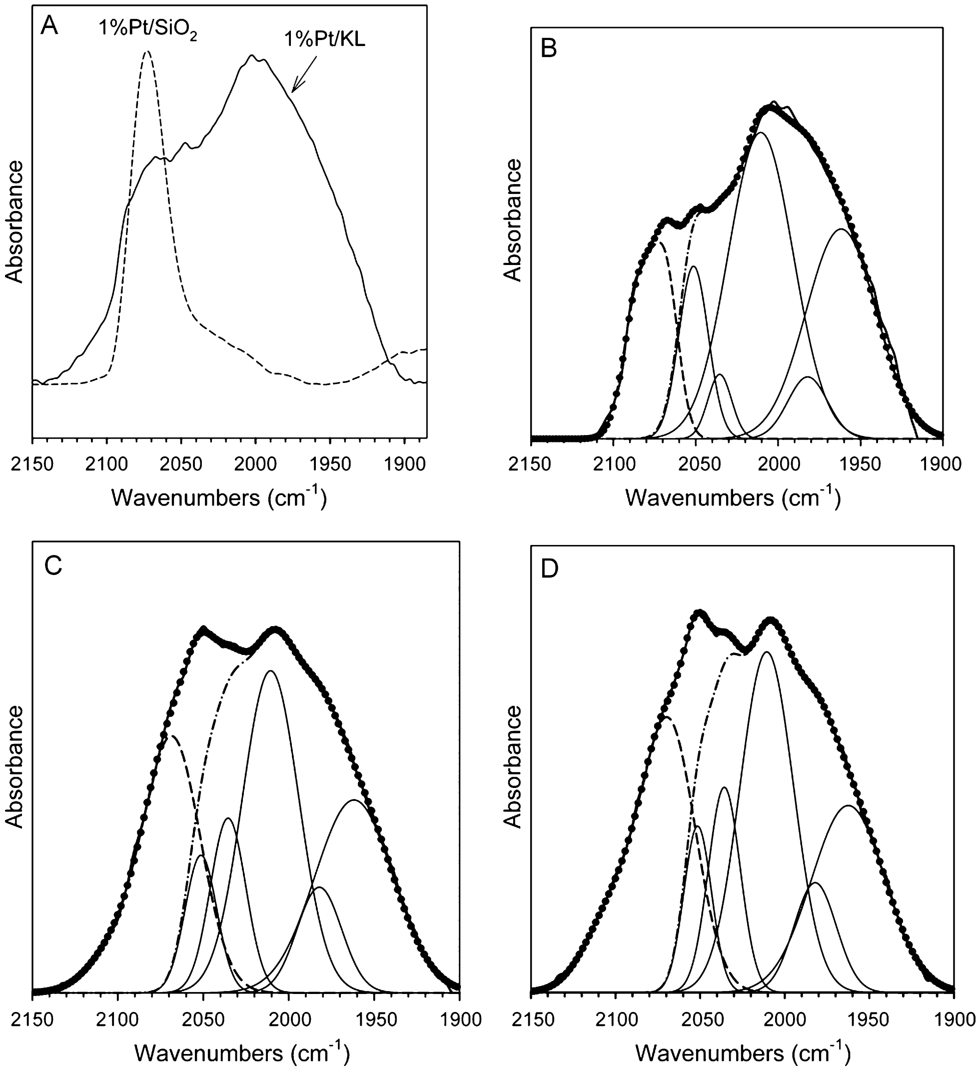

Fig. 2. (A) DRIFTS spectra for CO adsorption over 1%Pt/KL (solid line) and 1%Pt/SiO$_2$ (dashed line) at 40 °C. The catalysts were reduced at 600 °C in 75 ccm of 33%H$_2$/He, cooled to 40 °C in 50 ccm He, treated with 50 ccm of 2%CO/He for 30 min, and finally purged with He for 20 min. Note the height of the ν(CO) band for Pt/SiO$_2$ was divided by 3.8 to normalize. Gaussian fitting of ν(CO) for linearly bound CO (dashed, two components) and ν(CO) in Pt-carbonyls (dash-dotted, five components) for (B) 600 °C, (C) 500 °C and (D) 450 °C after similar treatments to (A).

well established in the literature [11,30,31] that a reaction exhibits a significant decrease in conversion when switching from a C–H label to the C–D label if the reaction involves C–H bond breaking in the rate limiting step due to the NKIE arising from the difference in bond energy. Therefore, the NKIE of 1.5 suggests the involvement of C–H bond activation in kinetically relevant steps. The degree of H–D exchange in the recovered propane when the reaction was conducted at 600 °C is shown in Fig. 3. There is hardly any H–D exchange between propane-d_0 and propane-d_8 or between the gaseous hydrocarbons and H_2/D_2 at the testing conditions suggesting that C–H bond activation is irreversible and hence all the propane chemically adsorbed on the Pt active sites completed the reaction to final products. When conducting the reaction at 500 °C (Table 3 and Fig. 4) or 400 °C (Table 4 and Fig. 5), the NKIE also exists with an average value of about 1.4 for both temperatures and with no significant H–D exchange in the recovered propane reactants. This indicates that C–H bond activation is the rate determining step for the dehydrogenation of propane over Pt/KL catalyst in this range of temperatures (400–600 °C).

Similarly, the NKIE exists when the propane dehydrogenation reaction, using an equimolar propane-d_0 and propane-d_8 mixture, was carried out on Pt/SiO$_2$ (Table 5) and no significant H–D

Table 2
Activity and selectivity results of dehydrogenation of propane over 1 wt% Pt/KL at 600 °C, 1 atm, and 2.6 h^{-1} WHSV using an equimolar propane-d_0 and propane-d_8 (25%C_3H_8/25%C_3D_8/balance He) mixture.

TOS (min)	$X_{C_3H_8}$ (C%)	$X_{C_3D_8}$ (C%)	k_H/k_D	$S_{Propene}$ (%)	$S_{Methane}$ (%)	S_{Ethene} (%)	S_{Ethane} (%)	$S_{Benzene}$ (%)
45	28.2	18.9	1.49	41	49	6	4	0.4
80	24.3	16.0	1.52	39	52	5	4	0.3
115	21.6	14.2	1.52	37	54	5	4	0.3
150	20.2	13.3	1.52	38	54	5	3	0.3
185	16.6	10.9	1.53	38	52	6	4	0.2
220	15.9	11.2	1.42	38	50	7	5	0.2

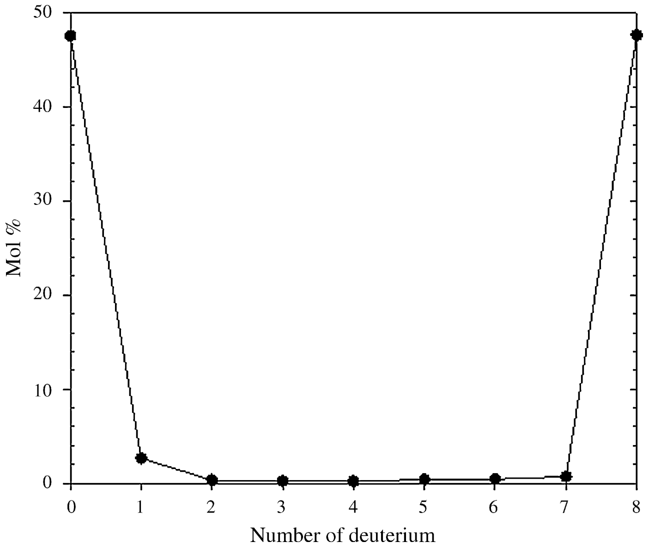

Fig. 3. Deuterium distribution in the recovered propane (equimolar feed of 25% propane-d_0/25% propane-d_8/balance He) during the dehydrogenation reaction over 1%Pt/KL at 600 °C, 1 atm, and WHSV of 2.6 h^{-1}.

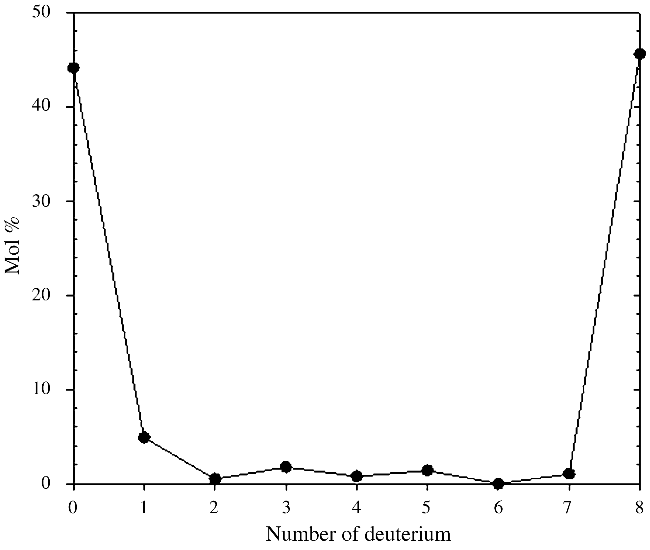

Fig. 4. Deuterium distribution in the recovered propane (equimolar feed of 25% propane-d_0/25% propane-d_8/balance He) during the dehydrogenation reaction over 1%Pt/KL at 500 °C, 1 atm, and WHSV of 2.6 h^{-1}.

exchange in the recovered propane was observed (Fig. 6). The NKIE (k_H/k_D) is almost constant with an average value of ∼2 and the catalyst deactivates with TOS. Comparing the performance of Pt/SiO$_2$ and Pt/KL catalysts during the dehydrogenation of equimolar propane-d_0 and propane-d_8 at 600 °C, both catalysts displayed an NKIE and severe catalyst deactivation with TOS, suggesting that the unique structure of KL-zeolite hardly influences catalyst performance during the propane dehydrogenation reaction.

The existence of NKIE at 400, 500, and 600 °C and the lack of H–D exchange in the recovered propane reactants at these temperatures suggest that (i) C–H bond activation is the rate determining step and (ii) entry of propane through the narrow windows of the L-zeolite to access the active Pt^0 sites (i.e., located on the Pt^0 crystallites residing within the wider lobes of the uni-axial channels of the L-zeolite) is relatively fast with respect to the surface reaction rate. This is in contrast with what we observed in the case of hexane dehydrocyclization over the same catalyst [16]. Since the entry rate of propane molecules through the narrow windows to access the active Pt^0 sites is faster than propane activation on the same sites, then the probability for bimolecular reactions increases; this may explain the high deactivation rate as a function of TOS. Indeed, significant deactivation of the catalysts with TOS was observed at 500 and 600 °C. For instance, at 600 °C, the $X_{C_3H_8}$ and $X_{C_3D_8}$ dropped from 28.2% to 18.9% at a TOS of 45 min to 15.9% and 11.2%, respectively, at a TOS of 220 min. To investigate the role of bimolecular reactions on catalyst deactivation, the analysis of carbon deposits by TPO was carried out for the used catalysts after 220 min of TOS under propane dehydrogenation at 600, 500, and 400 °C (Fig. 7). An intense CO$_2$ peak was observed from the TPO result of the spent catalyst for the reaction at 600 °C compared with ones conducted at 500 or 400 °C. The large amount of carbon deposited on the catalyst when the reaction was conducted at 600 °C relative to the 500 and 400 °C conditions leads to severe catalyst deactivation and may explain the lower activity of the catalyst at 600 °C. It seems that within the first 45 min in which the first sample was analyzed, some of the L-zeolite channels were rapidly blocked by carbon deposits and hence a fraction of the Pt active sites were lost during reaction testing at 600 °C. Furthermore, the carbon deposits formed by carrying out the reaction at 600 °C seem to be different (i.e., more reactive) compared to the carbon formed when the reaction was

Table 3
Activity and selectivity results for the dehydrogenation of propane over 1 wt% Pt/KL at 500 °C, 1 atm, and 2.6 h^{-1} WHSV using an equimolar propane-d_0 and propane-d_8 (25%C$_3$H$_8$/25%C$_3$D$_8$/balance He) mixture.

TOS (min)	$X_{C_3H_8}$ (C%)	$X_{C_3D_8}$ (C%)	k_H/k_D	$S_{Propene}$ (%)	$S_{Methane}$ (%)	S_{Ethene} (%)	S_{Ethane} (%)	$S_{Benzene}$ (%)
45	31.5	23.7	1.33	40	48	3	9	0.3
80	31.0	22.7	1.37	41	48	3	7	0.3
115	27.6	19.2	1.44	43	47	3	7	0.3
150	26.2	18.1	1.44	44	46	3	6	0.3
185	24.5	17.5	1.40	45	45	3	6	0.3
220	22.0	16.5	1.33	45	45	4	6	0.3

Table 4
Activity and selectivity results for the dehydrogenation of propane over 1 wt% Pt/KL at 400 °C, 1 atm, and 2.6 h^{-1} WHSV using an equimolar propane-d_0 and propane-d_8 (25%C$_3$H$_8$/25%C$_3$D$_8$/balance He) mixture.

TOS (min)	$X_{C_3H_8}$ (C%)	$X_{C_3D_8}$ (C%)	k_H/k_D	$S_{Propene}$ (%)	$S_{Methane}$ (%)	S_{Ethene} (%)	S_{Ethane} (%)	$S_{Benzene}$ (%)
45	6.0	4.4	1.36	52	37	1	9	0.3
80	6.5	4.5	1.43	55	35	2	8	0.0
115	7.0	5.1	1.36	57	33	2	8	0.0
150	6.6	4.7	1.41	59	32	2	7	0.0
185	6.7	4.7	1.42	60	31	2	7	0.0
220	6.7	4.8	1.40	61	31	2	7	0.0

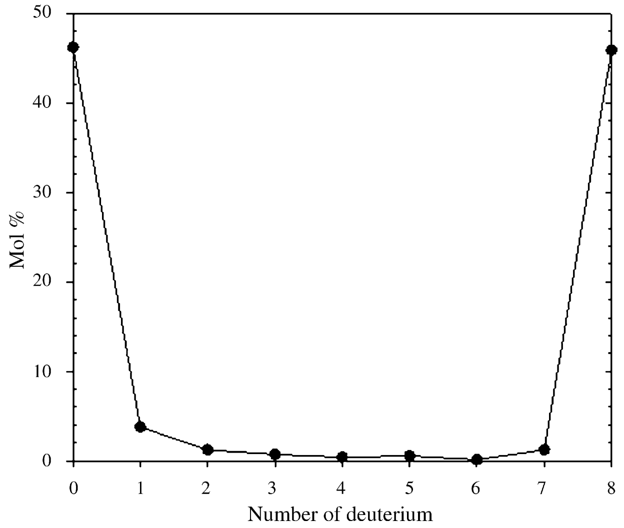

Fig. 5. Deuterium distribution in the recovered propane (equimolar feed of 25% propane-d_0/25% propane-d_8/balance He) during the dehydrogenation reaction over 1%Pt/KL at 400 °C, 1 atm, and WHSV of 2.6 h^{-1}.

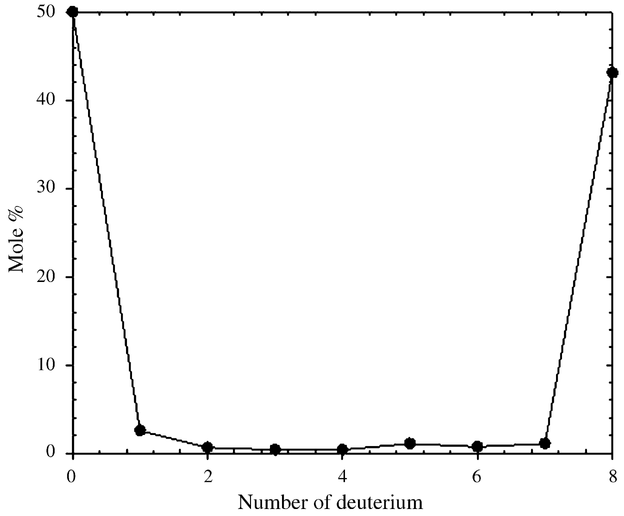

Fig. 6. Deuterium distribution in the recovered propane (equimolar feed of 25% propane-d_0/25% propane-d_8/balance He) during the dehydrogenation reaction over 1%Pt/SiO_2 at 600 °C, 1 atm, and WHSV of 2.6 h^{-1}.

conducted at 500 and 400 °C. We will not go into the details as to why this is the case, because it is outside the scope of this paper. Nevertheless, it is clear that carbon deposits play a significant role in catalyst deactivation due to the occurrence of bimolecular reactions on Pt sites (i.e., arising from the simultaneous contact of more than one propane molecule over Pt sites). In contrast to the case of hexane [16], the zeolite microstructure did not sufficiently control the entry and diffusion of propane molecules to the Pt sites relative to the Pt-catalyzed dehydrogenation of propane surface reaction.

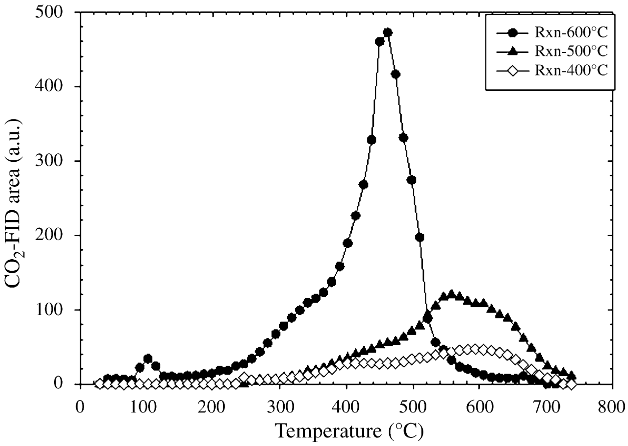

Fig. 7. Temperature programmed oxidation profiles (i.e., CO_2 – GC-FID areas) as a function of temperature for the used 1%Pt/KL catalysts using 1%O_2/He at 50 ml/min. The used catalysts were tested for the dehydrogenation of propane at 400, 500, or 600 °C prior to carrying out TPO.

There have been attempts to address the coking issue. The group of Dumesic [32,33] studied the dehydrogenation of isobutane reaction over Pt, PtSn and PtSnK catalysts supported on either silica or K-L-zeolite. The authors found that the PtSn/KL catalysts had significantly higher rates of isobutene production relative to PtSnK/silica. The authors suggested that Sn and K addition to Pt decreased coking by decreasing the ensemble size of Pt surface atoms, which in turn was suggested to inhibit the formation of coke precursors, the highly dehydrogenated surface species. Another possibility was that Sn facilitated transfer of coke to the support and away from active Pt sites. The high activity was suggested to be due to a stabilization of the molecularly adsorbed isobutane molecule by the zeolite, and by the assistance of K in facilitating isobutane dissociation.

When the dehydrogenation reaction was conducted at 300 °C, no activity was observed. However, the H–D exchange between propane-d_0 and propane-d_8 (Fig. 8) was more pronounced compared with the H–D exchanges when the reaction was conducted at 400, 500, or 600 °C. The occurrence of H–D exchange at 300 °C and the lack of exchange at 400, 500, or 600 °C indicates a change from reversible adsorption at lower temperature to irreversible adsorption and subsequent reaction at temperatures higher than 400 °C. This can be explained by considering the energy diagram presented in Scheme 1. At low temperature, adsorption of propane is reversible, as the large activation energy barrier for double bond formation prevents further reaction. However, single bond activation and exchange with the surface hydrogen pool does occur at low temperature, and is a well-established process [34,35]. Chrysostomou et al. [36] investigated the thermal activation of propyl groups on Pt(1 1 1) and in one experiment, carried out TPD-MS of 1 and 2-propyl groups (5 L) adsorbed on a Pt(1 1 1) surface pretreated with 20 L of deuterium. At −23 °C, they observed a TPD feature for both propyl intermediates, with all fragments up to C_2D_5+, indicating multiple H–D exchanges in individual molecules, up to

Table 5

Activity and selectivity results for the dehydrogenation of propane over 1 wt% Pt/SiO_2 at 600 °C, 1 atm, and 2.6 h^{-1} WHSV using an equimolar propane-d_0 and propane-d_8 (25%C_3H_8/25%C_3D_8/balance He) mixture.

TOS (min)	$X_{C_3H_8}$ (C%)	$X_{C_3D_8}$ (C%)	k_H/k_D	$S_{Propene}$ (%)	$S_{Methane}$ (%)	S_{Ethene} (%)	S_{Ethane} (%)	$S_{Benzene}$ (%)
45	15.4	7.8	1.98	66	20	10	2	0.5
80	11.2	5.6	2.01	64	21	13	1	0.9
115	7.6	3.2	2.36	59	24	16	1	0.3
150	7.1	3.2	2.24	55	25	18	1	0.3
185	7.0	3.5	1.97	53	26	20	1	0.0
220	7.1	3.7	1.89	51	27	21	1	0.0

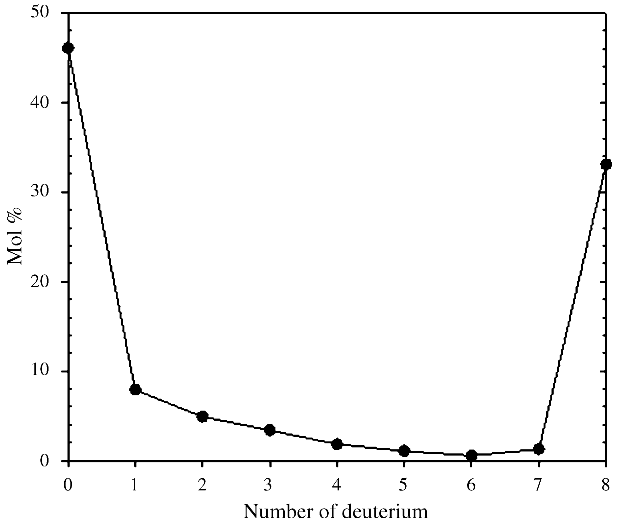

Fig. 8. Deuterium distribution in the recovered propane (equimolar feed of 25% propane-d_0/25% propane-d_8/balance He) during the dehydrogenation reaction over 1%Pt/KL at 300 °C, 1 atm, and WHSV of 2.6 h^{-1}.

and including propane-d_8. This led the authors to conclude that a cyclic adsorbed propyl-propene-propyl surface reaction took place, with the 1-propyl species responsible for exchanging hydrogens at the central carbon atom, and the 2-propyl species responsible for exchanging end carbons.

At higher temperatures it is proposed that the activation energy barrier for dehydrogenation is shifted lower; in this case, exchange with the surface pool of hydrogen ceases, as the adsorbed propane species rapidly dehydrogenates. At this point, adjacent adsorbed propene molecules can react to form coke.

It is well established that the rate of isotope exchange relative to the rate of dehydrogenation reaction decreases and, as a consequence, causes the degree of exchange to increase as the temperature decreases [10]. For instance, Shi and Davis [10] reported that the H–D exchange between methylcyclohexane-d_{14} and octane-d_0 achieved almost equilibrium over Pt/SiO_2 catalyst at 300 °C but not at 482 °C. Although H–D exchange occurs between propane-d_0 and propane-d_8 (see Fig. 8), it is far from equilibrium, indicating some influence of the structure of the L-zeolite on restricting propane molecules to Pt sites at lower temperature (300 °C).

Finally, comparing the selectivities of the products during the dehydrogenation of propane over the Pt/KL catalyst at 600, 500, and 400 °C (Tables 2–4), a selectivity to propene in the range of 40–60% was obtained at the tested tempertatures. The high selectivity of methane combined with the low selectivities of ethane, ethene, and benzene indicate that the dehydrogenation reaction is combined with cracking, β-scission, and dehydrocyclization (with very low activity) reactions.

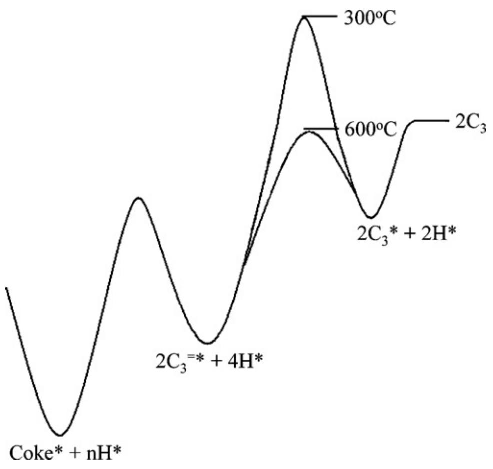

Scheme 1.

4. Conclusions

Hydrogen chemisorption and DRIFTS revealed that the majority of Pt clusters are ultra-small and well dispersed within the channels of L-zeolite when the catalyst was prepared using the CVD method. The existence of an NKIE (1.4–1.5) and the lack of H–D exchange for the conversion of an equimolar mixture of propane-d_0 and propane-d_8 over 1%Pt/KL catalyst at temperatures of 400, 500, and 600 °C and 1 atm, suggests that the adsorption of propane on Pt sites is irreversible and that C–H bond activation is the rate determining step for the dehydrogenation reaction of propane at these conditions. In contrast to the case of hexane aromatization, the unique structure of L-zeolite did not sufficiently inhibit bimolecular reactions to prevent catalyst deactivation for propane dehydrogenation. At 300 °C, the H–D exchange between propane-d_0 and propane-d_8 was more pronounced, suggesting that the adsorption of propane is switched from irreversible to reversible at lower temperature.

References

[1] C.H. Bartholomew, R.J. Farrauto, Fundamentals of Industrial Catalytic Processes, John Wiley & Sons, New Jersey, 2006, pp. 534–554.
[2] N.R. Shiju, V.V. Guliants, Appl. Catal. A 356 (2009) 1–17.
[3] O.A. Bariås, A. Holmen, E.A. Blekkan, Catal. Today 24 (1995) 361–364.
[4] T. Waku, J.A. Biscardi, E. Iglesia, J. Catal. 222 (2004) 481–492.
[5] M.S. Kumar, A. Holmen, D. Chen, Micropor. Mesopor. Mater. 126 (2009) 152–158.
[6] P.L. de Cola, R. Gläser, J. Weitkamp, Appl. Catal. A 306 (2006) 85–97.
[7] M.S. Kumar, D. Chen, J.C. Walmsley, A. Holmen, Catal. Commun. 9 (2008) 747–750.
[8] P. Andy, M.E. Davis, Ind. Eng. Chem. Res. 43 (2004) 2922–2928.
[9] D. Akporiaye, S.F. Jensen, U. Olsbye, F. Rohr, E. Rytter, M. Rønnekleiv, A.I. Spjelkavik, Ind. Eng. Chem. Res. 40 (2001) 4741–4748.
[10] B. Shi, B.H. Davis, J. Catal. 147 (1994) 38–47.
[11] B. Shi, B.H. Davis, Stud. Surf. Sci. Catal. 101 (1996) 1145–1154.
[12] B. Shi, B.H. Davis, J. Catal. 168 (1997) 129–132.
[13] J.A. Bicardi, E. Iglesia, Catal. Today 31 (1996) 207–231.
[14] S.D. Jackson, J. Grenfell, I.M. Matheson, G. Webb, Stud. Surf. Sci. Catal. 122 (1999) 149–155.
[15] J.A. Biscardi, E. Iglesia, J. Catal. 182 (1999) 117–128.
[16] K.G. Azzam, G. Jacobs, W. Shafer, B.H. Davis, J. Catal. 270 (2010) 242–248.
[17] J.M. Hill, R.D. Cortright, J.A. Dumesic, Appl. Catal. A 168 (1998) 9–21.
[18] R.D. Cortright, J.A. Dumesic, Appl. Catal. A 129 (1995) 101–115.
[19] G. Jacobs, W.E. Alvarez, D.E. Resasco, Appl. Catal. A: Gen. 206 (2001) 267–282.
[20] G. Jacobs, F. Ghadiali, A. Pisanu, A. Borgna, W.E. Alvarez, D.E. Resasco, Appl. Catal. A 188 (1999) 79–98.
[21] M. Ballatreccia, R. Zanoni, C. Dossi, R. Psaro, S. Recchia, G. Vlaic, J. Chem. Soc. Faraday Trans. 91 (1995) 2045–2049.
[22] E. Mielczarski, S.B. Hong, M.E. Davis, J. Catal. 134 (1992), 349–358 and 359–369.
[23] F. Ghadiali, G. Jacobs, A. Pisanu, A. Borgna, W.E. Alvarez, D.E. Resasco, Stud. Surf. Sci. Catal. 130 (2000) 2537–2542.
[24] G. Larsen, G.L. Haller, Catal. Lett. 3 (1989) 103–110.
[25] G. Jacobs, F.A. Ghadiali, A.M. Pisanu, A. Borgna, W.E. Alvarez, D.E. Resasco, Appl. Catal. 188 (1999) 79.
[26] M.M.J. Treacy, Micropor. Mesopor. Mater. 28 (1999) 271.
[27] G. Jacobs, F.A. Ghadiali, C. Padro, A. Borgna, W.E. Alvarez, D.E. Resasco, J. Catal. 191 (2000) 116.
[28] A. Yu Stakheev, E.S. Shpiro, N.I. Jaeger, G. Schulz-Ekloff, Catal. Lett. 34 (1995) 293–303.
[29] A. Yu Stakheev, E.S. Shpiro, N.I. Jaeger, G. Schulz-Ekloff, Stud. Surf. Sci. Catal. 98 (1995) 108–109.
[30] H.A. Dabbagh, T.S. Huang, B. Franzus, B.H. Davis, Tetrahedron 47 (1991) 949–960.
[31] A. Ozaki, Isotopic Studies of Heterogeneous Catalysis, Academic Press, New York, NY, 1977.
[32] J.M. Hill, R.D. Cortright, J.A. Dumesic, Appl. Catal. A: Gen. 168 (1998) 9.
[33] R.D. Cortright, J.A. Dumesic, Appl. Catal. A: Gen. 129 (1995) 101.
[34] A. Farkas, Trans. Faraday Soc. 36 (1940) 522.
[35] J.A. Oliver, C. Kemball, R. Brown, E.W. Jamieson, J. Chem. Soc., Faraday Trans 1: Phys. Chem. In Condensed Phases 81 (1985) 1871.
[36] D. Chrysostomou, C. French, F. Zaera, Catal. Lett. 69 (2000) 117.